DOI 10.1002/pmic.200500149

RESEARCH ARTICLE

Kinetics of antigen binding to antibody microspots: Strong limitation by mass transport to the surface

Wlad Kusnezow[1], Yana V. Syagailo[1], Sven Rüffer[1], Konstantin Klenin[2], Walter Sebald[3], Jörg D. Hoheisel[1], Christoph Gauer[4] and Igor Goychuk[5]

[1] Division of Functional Genome Analysis, Deutsches Krebsforschungszentrum, Heidelberg, Germany
[2] Division of Biophysics of Macromolecules, Deutsches Krebsforschungszentrum, Heidelberg, Germany
[3] Department of Physiological Chemistry II, Biocenter, University of Würzburg, Würzburg, Germany
[4] Advalytix AG, Brunnthal, Germany
[5] Institute of Physics, University of Augsburg, Augsburg, Germany

Received: March 10, 2005
Revised: June 17, 2005
Accepted: June 27, 2005

It is well documented that diffusion has generally a strong effect on the binding kinetics in the microtiter plate immunoassays. However, a systematic quantitative experimental evaluation of the microspot kinetics is still missing in the literature. Our work aims at filling this important gap of knowledge on the example of antigen binding to antibody microspots. A mathematical model was derived within the framework of two-compartment model and applied to the quantitative analysis of the experimental data obtained for typical antibody microspot assays. A strong mass-transport dependence of the antigen-antibody microspot kinetics was identified to be one of the main restrictions of this new technology. The binding reactions are slowed down in the microspot immunoassays by several orders of magnitude as compared with the corresponding well-stirred bulk reactions. The task to relax the mass-transport limitations should thus be one of the most important issues in designing the antibody microarrays. These limitations notwithstanding, the detection range of more than five orders of magnitude and the high sensitivity in the low femtomolar range were experimentally achieved in our study, demonstrating thus an enormous potential of this highly capable technology.

Keywords:
Antibody microarray / Mass-transport limited reaction / Microspot kinetics / Two-compartment model

1 Introduction

The ambient analyte theory [1, 2] provides a reasonable foundation for understanding the performance of modern microarray immunoassays. This theory is based on the law of mass action and predicts a much higher sensitivity of microspot multi-analyte assays versus conventional ELISAs. Assuming a scanner resolution of about 0.1 Cy-dye molecules/μm^2 (cf. www.perkinelmer.com), the sensitivity of microarrays made of high-affinity antibodies (10^{-9}–10^{-12} M) has to be in the attomolar to zeptomolar range according to this theory. However, the today's sensitivities achieved for antibody microarrays are still far from this theoretical limit and stay usually in the nano- to picomolar range if direct protein labeling is applied [3, 4]. This discrepancy between the experiment and the theory was attributed to a number of causes, such as the high complexity and low stability of proteins in general [3, 5], the low affinity and specificity of the antibodies investigated [6–8], as well as the low sensitivity of the detection methods [3] or an enhanced level of the background noise, which is intrinsic to antibody microarray technology itself [4, 7, 8].

Correspondence: Dr. Wlad Kusnezow, Division of Functional Genome Analysis, Deutsches Krebsforschungszentrum, Im Neuenheimer Feld 580, D-69120 Heidelberg, Germany
E-mail: w.kusnezow@dkfz.de
Fax: +49-6221-424-687

Abbreviations: GPTS, (3-glycidoxypropyl)trimethoxy-silane; **IFNG**, interferon-gamma; **KLH**, keyhole limpet hemocyanin; **TCM**, two-compartment model; **TG**, thyroglobulin

While a strong dependence of the microtiter plate immunoassays on diffusion is well documented [9], some recent studies of the protein microarrays have found that the antigen binding kinetics to the antibody microspot assays might be reaction rather than diffusion limited [9–11]. However, in these studies the association and dissociation rates of the analyzed analyte molecules have not been measured independently. It is also known from the experimental research of the DNA-microarrays that stirring may improve the signal development on a chip by a factor of up to ten [12–14]. Therefore, the DNA-microspot reactions are strongly diffusion limited and there are no convincing reasons to believe that the protein microarrays are much different in this respect.

The detailed knowledge of the reaction mechanisms would enable us to predict the reaction duration as well as to estimate realistically the sensitivity and other parameters of the microarrays. This in turn would allow one to disclose and formulate the basic principles of the optimal design and development of antibody microarrays. Profound investigations of this basic issue are still missing in the protein microarray literature. The role of the mass-transport dependence in the microspot reaction kinetics has not been analyzed in quantitative terms thus far. This study presents one of the first attempts to fill this gap and to shed light on the overall reaction mechanisms in the protein microarrays.

Starting with common considerations of ideal mass-transport independent kinetics, we develop also a convenient mathematical tool within the framework of the two-compartment model (TCM) [15–18]. The TCM has been originally proposed for the analysis of mass-transport limited bimolecular interactions in the Biacore instruments. This relatively simple model dissects the mass transport dependent binding into the two steps: (i) the transport of the analyte from the bulk compartment to the surface reaction area (reaction compartment) and (ii) the subsequent binding process. The overall kinetics is correspondingly described by a system of two coupled nonlinear differential equations that reduces to a single nonlinear differential equation upon adiabatic elimination of one variable in a steady state approximation. The TCM-based mathematical model enables us to estimate the degree of mass-transport dependence, duration of the antibody microspot reaction and to draw conclusions about the consequences of the obtained parameters on the technology development and application. We also analyzed an antibody microspot assay, which is similar to set-ups that are commonly produced and processed in other microarray laboratories, so that the parameters obtained in this study can be easier generalized. Using direct protein labeling, we demonstrated the enormous capacity of the antibody microarray technology.

2 Materials and methods

2.1 Materials

Untreated slides were purchased from Menzel-Gläser (Braunschweig, Germany). Milk powder, (3-glycidoxypropyl)trimethoxy-silane (GPTS), recombinant human interferon-gamma (IFNG) anti-human IFNG mAb (anti-IFNG) keyhole limpet hemocyanin (KLH) and affinity isolated anti-hemocyanin antibody (anti-KLH) were obtained from Sigma-Aldrich (Munich, Germany). Thyroglobulin (TG) and anti-thyroglobulin mAb (anti-TG) were from Hy-Test Ltd. (Turku, Finland).

2.2 Fabrication of antibody arrays

Homemade epoxysilanized slides were manufactured according to the following protocol: untreated slides were washed with 100% ethanol, then etched overnight by immersion in 10% NaOH, cleaned by sonication in the same solution for 15 min, rinsed four times in water, washed twice in ethanol and derivatized in a 100% GPTS solution at room temperature for 3 h. After silanization, GPTS-treated slides were washed thoroughly with dichloroethane and dried with nitrogen. PBS buffer supplemented with 0.5% trehalose was used as spotting buffer. The antibodies were spotted using a SDDC-2 Micro-Arrayer of Engineering Services (Toronto, Canada) and SMP2 pins (TeleChem, Sunnyvale, CA). After spotting, the slides were incubated at 4°C overnight and subsequently blocked for 3 h at room temperature in PBST (0.05% Tween20) supplemented with 4% milk powder.

2.3 Antigen labeling and incubation

Antigen solution of 1 mg/mL was labeled with the monofunctional Cy3-dye NHS-ester (Amersham Biosciences, Freiburg, Germany) as recommended by the manufacturer. Unreacted dye was separated from the labeled proteins by PD-10 columns (Sephadex™ G-25, Amersham Biosciences). Incubation of the microarrays with antigens occurred in Flexiperms. The Flexiperms were of 3.3-mm well radius and 10-mm height and fixed on the slide surface using double-adhesive tape. Every incubation chamber contained only one spot in the middle of the reaction well bottom (Fig. 1C). This enabled us to avoid any influence on kinetics by neighboring spots. All incubations were performed with 100 μL of antigen solution both without mixing and with mixing using the SlideBooster (Advalytix, Brunnthal, Germany) [14]. The SlideBooster agitation protocol was optimized by visually observing the dispersion of the CresolRed in the solution. This enabled us to achieve homogenous color dispersion in a well after only a couple of seconds. After the incubation, the slides were rinsed several times with PBST.

2.4 Scanning and data analysis

Fluorescence signals were recorded using a ScanArray 5000 unit (Packard, Billerica, USA) and analyzed with the GenePix software package (Axon Instruments, Union City, USA). The results were stored and managed in an appropriate Microsoft Access database. All data points in this work represent an average of four to six individual measurements obtained from at least two slides. The signal intensities obtained at

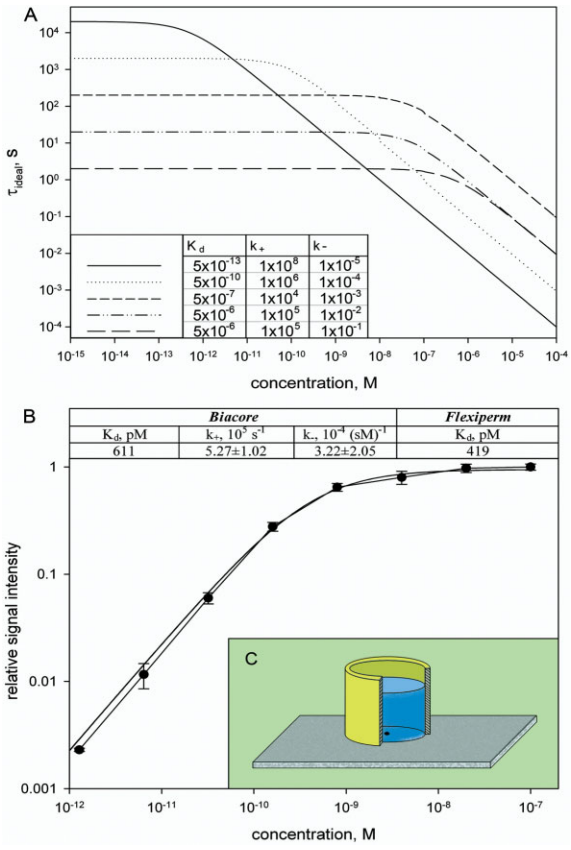

Figure 1. (A) Ideal characteristic time τ_{ideal} for different antibodies plotted against analyte concentration. The simulation was carried out with hypothetical affinity parameters of antibodies, K_d, k_+ and k_- (see panel on the graph). (B) k_+, k_- and K_d constants derived from Biacore measurements (see table above) as well as K_d obtained after 30 h incubation in Flexiperm under stirring condition. The signal intensities were normalized against the maximal signal intensity at 100 nM IFNG. (C) Depiction of the experimental assembly used for this study: well-like incubation chambers were affixed on the surface of the slides, so that every well chamber contained only one spot in the central position.

different scanner adjustments were first converted into comparable values using previously obtained factors of signal intensification at different laser powers and PMT of the scanner. The relative change of signal intensities was calculated as $dS(t)\,/\,dt \approx (S_{i+1} - S_i)/(t_{i+1} - t_i)$ with $S_{i+1} - S_i$ being the difference between two subsequent signal intensities recorded at t_{i+1} and t_i, respectively. All fittings and simulations were done using SigmaPlot. Within the TCM [15, 16], the binding kinetics can be described in the steady-state approximation by the following nonlinear differential equation:

$$\frac{dS(t)}{dt} = \frac{k_+ L_0 (S_{\max} - S(t)) - k_- S(t)}{1 + k_+ (S_{\max} - S(t))/k_m}. \quad (1)$$

In Eq. (1), k_+ (in $(\mathrm{Ms})^{-1}$) and k_- (in Ms^{-1}) are the association and dissociation rate constants, respectively; L_0 is the initial analyte concentration (in M); S_{max} and S are the maximum and current signal intensities expressed in signal units (SU), and k_m is the phenomenological mass transport constant (in SU/(Ms)). Additionally, $S_{max} = \alpha[A]$ and $S = \alpha[AL]$, where $[A]$ is antibody surface concentration, $[AL]$ surface concentration of antibody/antigen complexes (both in mol/cm^2) and α is a proportionality coefficient (SU* cm^2/mol). It should be noticed that S is numerically equal to the fractional occupancy of binding sites in our analysis, so that $S_{\max} = 1$.

3 Results

3.1 Diffusion-independent hybridization kinetics

In the absence of diffusion limitations or any other disturbing factors, like steric hindrance or heterogeneity of affinity due to immobilization and under the so-called ambient analyte conditions, *i.e.* when the depletion of the initial antigen bulk concentration L_0 due to its binding to antibodies is practically negligible [1, 2], the underlying kinetics has an ideal, pseudo-first order character and the signal grows exponentially in time. In such a case, the maximal sensitivity of the antibody microarray can be achieved. The corresponding ideal exponential kinetics is described by the following equation:

$$S(t) = S_\infty (1 - \exp(-t/\tau_{\mathrm{ideal}})) \quad (2)$$

$$\tau_{\mathrm{ideal}} = 1/(k_- + k_+ L_0), \quad (3)$$

where τ_{ideal} is the characteristic time of ideal binding kinetics (in *s*). This is the time required for the signal to develop from zero to about 63% of its maximal possible value $S_\infty = S_{\max} L_0/(L_0 + K_d)$. Here, $K_d = k_-/k_+$ is the equilibrium dissociation constant with k_+ and k_- being the binding and dissociation rate constants, correspondingly. According to Eq. (3), τ_{ideal} equals approximately $1/k_+ L_0$ for $L_0 \gg K_d$. Hence, it is inversely proportional to the analyte concentration L_0. On the other hand, if $L_0 \ll K_d$ τ_{ideal} equals approximately to $1/k_-$ and it does not depend on the analyte concentration anymore in this limit. Consequently, the affinity parameters of a receptor (antibody) molecule present a key factor, if the microspot binding kinetics is mass-transport independent (Fig. 1A). Moreover, the incubation time required to reach the equilibrium for an analyte/receptor system would still differ by many orders of magnitude depending on the antigen concentration L_0. It is also evident from Eqs. (2) and (3) as well as from Fig. 1A that the development of signal intensities at initial incubation times occurs proportionally to $S_{\max} L_0 k_+$ for all analyte concentrations. A correlation of signal with K_d of a ligand/receptor pair can therefore be expected only near the reaction equilibrium for a sufficiently long observation time.

3.2 Establishment of a test system

In preparative work, a number of different antibodies against KLH, TG and IFNG were tested. The fastest and most reproducible progression curves were observed for the anti-IFNG. For this reason, this antibody was used for all work described in this publication unless stated otherwise. In addition, different incubation geometries were tested. The classical microtiter plate (MTP) well geometry was found to yield the highest signal intensities and it was consequently used for all experiments shown here (Fig. 1C).

The establishment of ambient analyte conditions in the absence of any other disturbing factor except for a mass-transport limitation is a prerequisite for the TCM-based analysis (see Eq. (1)). The fraction of the analyte molecules bound to the antibody spot from the bulk solution is obviously $f = [AL]\pi R^2/L_0V$, where R is the spot radius in cm and V is the incubation volume in cm^3. In accordance with Eq. (2), the maximal value of f (at equilibrium) is $f_{max} = [A]\pi R^2/(L_0+K_d)V$. Therefore, for $L_0 \ll K_d$ (our goal is to detect as small analyte concentrations as possible), $f_{max} \approx [A]\pi r^2/K_dV$ and it does not depend on the analyte concentration at all. It must be $f_{max} \ll 1$ for the ambient analyte condition to be established. We checked this condition, *i.e.* $[A]\pi R^2 \ll K_dV$, for our system by (i) measuring the affinity of anti-IFNG and (ii) estimation of the binding site density.

The affinity parameters of anti-IFNG ($k_+ = (5.27 \pm 1.02) \times 10^5$ (Ms^{-1} and $k_- = (3.22 \pm 2.05) \times 10^{-4}\ Ms^{-1}$) had been obtained on a Biacore system (not shown). They could be verified by incubating slides of anti-interferon spots for about 30 h with a dilution series of interferon concentrations, ranging from 100 nM to 1 pM (Fig. 1B). Binding affinity constants were obtained in this experiment by fitting the experimental data to the equation $S_\infty = S_{max}L_0 / (L_0 + K_d)$, which describes the dependence of the signal intensity on the analyte concentration under thermodynamic equilibrium. The obtained K_d values of 611 pM (Biacore) and 419 pM (incubation) were in good agreement. Due to this fact, the potential disturbing factors like steric hindrance or heterogeneous affinity can be assumed insignificant in our system.

To evaluate the number of antibodies bound to a spot, anti-IFNG of known concentration was labeled with Cy3 and spotted using differently sized pins (data not shown). One part of the slides was immediately scanned, the other part was processed as usually (overnight incubation, blocking). Estimated from the difference of signal intensities between the freshly spotted and treated slides, about 40% of the antibody was bound to the surface at optimal spotting concentrations of 1 mg/mL. Since the delivery volume of SMP2 pins is 0.5 nL as indicated by the manufacture (www.arrayit.com) and spot size about 90 μm as obtained from our database, approximately 2×10^5 binding sites/μm^2 are bound to the spot. However, due to random orientation as well as partial denaturation of antibodies, the number of active binding sites/μm^2 would be lower at least two times or even more. Based on the obtained parameters, SMP2 pins satisfy for our setup the ambient analyte condition ($[A]\pi R^2 \approx 0.01K_dV$) and consequently they were used for spotting in all subsequent experiments.

3.3 Quantitative assessment of mass-transport dependency using the classical two-compartment theory

Because all above considerations refer only to ideal kinetics, the reaction duration may be significantly prolonged due to a mass-transport dependence. To investigate this issue, slides were incubated with five different antigen concentrations, 100 nM, 20 nM, 4 nM, 800 pM and 160 pM, and the signal intensities were measured after different times of 10 min to a maximum of 24 h. The obtained signal intensities were normalized against the maximum signal intensity at 100 nM antigen concentration.

Using TCM, data obtained at analyte concentrations within three orders of magnitude and under stirring conditions could be successfully fitted (see Eq. (1)). The experimentally determined mean mass transport constant under stirring condition was $k_m = (1.31 \pm 0.15) \times 10^4$ SU/(MS) (Fig. 2A). Under non-stirring condition, the variation of the signal intensities, especially at low analyte concentrations, was much higher. The corresponding k_m (Fig. 2B) could therefore only be roughly estimated (about 3200 SU/(MS)). Strong variability of signal intensities was also observed under stirring conditions but only at sufficiently low analyte concentrations of several picomolar.

Since the reaction occurs faster at high analyte concentrations, the impact of stirring is relatively small even for short incubation times (Fig. 3). At low analyte concentrations, a maximal four- to fivefold increase in the signal intensity was observed and the gain remained almost unchanged during the time course of binding reaction, even for an incubation time as long as 22 h. The k_m value obtained under non-stirring conditions can also be estimated using the following consideration. According to Eq. (1), both $dS(t)/dt$ and the absolute signal intensity should be directly proportional to k_m, if $k_+ S_{max} \gg k_m$ and $S_{max} \gg S$. Since these inequalities hold in our case, k_m under the non-stirring conditions must be about four times lower than under the stirring conditions.

3.4 Analytical solution of two-compartment model

To fit directly the progression curves measured experimentally, we brought the TCM into a new form allowing for a convenient analysis of microarray data. For the initial condition $S(0) = 0$, we found the solution of Eq. (1) in the closed analytical form reading:

$$S(t) = S_\infty(1 - W[c\exp(-\Gamma t)]/W[c]), \quad (4)$$

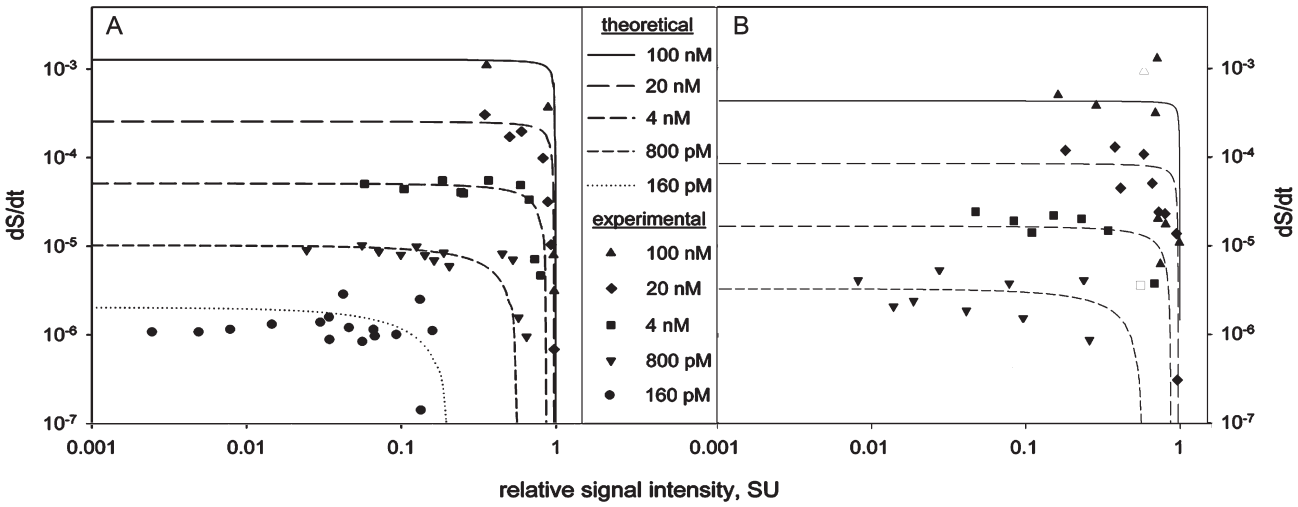

Figure 2. Signal development *dS(t)/dt* versus relative signal intensity *S* under the stirring (A) and non-stirring (B) conditions. Fittings were done according to Eq. (1), using the affinity parameters obtained from the Biacore measurements.

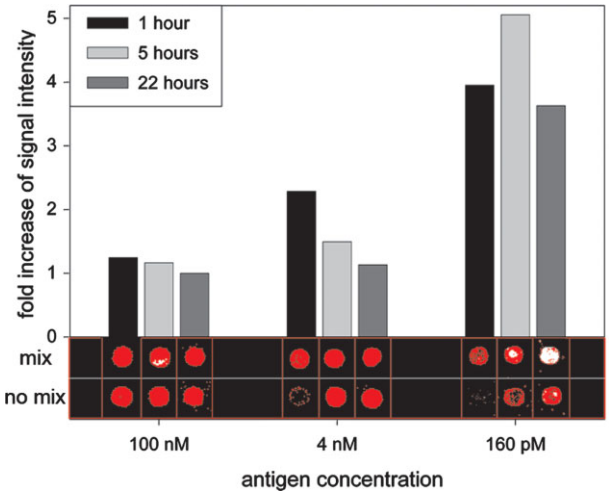

Figure 3. Relative increase of signal intensity due to stirring. Data for three different analyte concentrations are presented after 1-, 5- and 22-h incubations. The corresponding spot scans (at similar scanner adjustment for every concentration) are depicted in a pseudo-color scale for stirring (upper row) and non-stirring (lower row) conditions.

where W(x) is the Lambert special function defined as the solution of the equation $W(x)\exp[W(x)] = x$ [19]. Furthermore, in Eq. (4)

$$\Gamma = \frac{k_- + k_+ L_0}{1 + \frac{k_- S_{\max}}{k_m(K_d + L_0)}} \tag{5}$$

is the rate of approaching the steady state (this rate interpretation holds true, if the parameter is small, $c \ll 1$, see below). Furthermore, $c = a\exp(a)$ where

$$a = \frac{k_+ L_0 S_{\max}}{k_- S_{\max} + k_m(K_d + L_0)}, \tag{6}$$

is a dimensionless parameter, which measures the deviation of the kinetics in Eq. (4) from an ideal single-exponential kinetics. Since $W(x) \approx x$ for $x \ll 1$, Eq. (3) yields a single-exponential kinetics for $a \ll 1$:

$$S(t) = S_\infty(1 - \exp(-\Gamma t)). \tag{7}$$

Moreover, Eq. (5) can be transformed to:

$$\frac{1}{\Gamma} = \frac{1}{\Gamma_{\text{ideal}}} + \frac{1}{\Gamma_m}, \tag{8}$$

where $\Gamma_{\text{ideal}} = k_- + k_+ L_0$ is the rate of ideal kinetics and

$$\Gamma_m = k_m \frac{(L_0 + K_d)^2}{K_d S_{\max}} \tag{9}$$

is the rate constant related to the mass transport. Eq. (8) allows for a simple interpretation: the overall time constant of the binding reaction $\tau \equiv 1/\Gamma$ equals the sum of the time constant of the ideal reaction kinetics $\tau_{\text{ideal}} \equiv 1/\Gamma_{\text{ideal}}$ and the time constant of the mass transport $\tau_m \equiv 1/\Gamma_m$, *i.e.*, $\tau = \tau_{\text{ideal}} + \tau_m$.

The inverse dependence allowing calculating the time that is required to reach the signal intensity of $S(t)$ or the fractional occupancy $S(t)/S_\infty$ can be derived from Eq. (1) after its integration. This yields

$$\Gamma t = a\frac{S(t)}{S_\infty} - \ln\left(1 - \frac{S(t)}{S_\infty}\right) \tag{10}$$

with a given in Eq. (6) and Γ in Eq. (5). For $S(t) \ll S_\infty$, one finds from Eq. (10) that the initial development of signal intensity over time is linear

$$S(t) \approx \frac{S_\infty \Gamma}{1 + a} t = S_{\max} v_0 t, \tag{11}$$

where the initial binding reaction velocity v_0 is introduced. One can show that $1/v_0 = 1/v_{\text{ideal}} + 1/v_m$, where $v_{\text{ideal}} = k_+ L_0$ is the ideal initial binding velocity and $v_m = k_m L_0 / S_{\max}$

is the mass transport contribution. Note that $v_0 \approx v_m$ in the case of mass transport limited binding with $v_m \ll v_{ideal}$.

3.5 Two-compartment approach for the analysis of microspot reactions: A case study

To demonstrate the applicability of our approach, the reaction kinetics was analyzed for an example of IFNG antigen-antibody pair. The previously extracted mass transport constants indicate that the overall reaction rate on anti-IFNG spot under non-stirring and even stirring conditions is strongly limited by mass transport, since $\Gamma \approx k_- k_m/(k_+ S_{max}) \ll k_-$ and $k_m \ll k_+ S_{max}$. The ratio of the maximal ideal forward reaction rate to the rate of material transport flux, $\phi = k_+ S_{max} / k_m$, being the factor indicating the slowing down of the ideal kinetics, is about 40 and 160 for stirring and non-stirring conditions, respectively. The increase of ϕ leads to the proportional increases of the incubation time required for an anticipated fractional occupancy on the spot, which can be estimated in accordance with Eq. (10). Upon calculating the times needed to reach 50% of the maximum steady-state signal intensity $(S(t)/S = 0.5)$ for analyte concentrations over K_d, we found these corresponding times to agree with the data obtained experimentally (Fig. 4A and B). They vary from

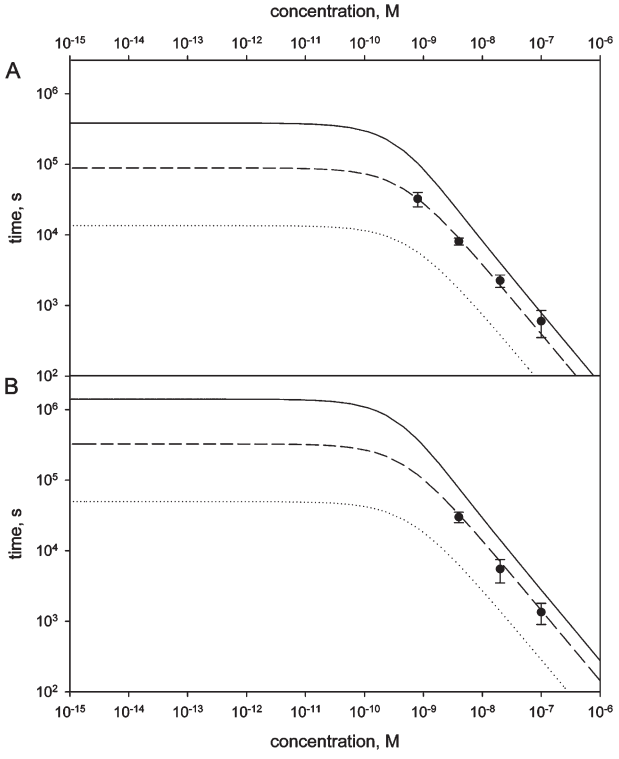

Figure 4. Dependence of the time required to reach 10% (···), 50% (– –) and 95% (– –) of the maximal signal intensity under stirring (A) and non-stirring (B) conditions. Calculations are done in accordance with Eq. (10) using the values k_m obtained experimentally. Data points (●) indicate the half-maximum saturation of signal intensities observed experimentally.

a few dozen minutes until several hours. The same times for $L_0 \ll K_d$ are about 25 and 100 h with and without stirring, respectively. Lower fractional occupancy results in a proportional reduction of the required times (*e.g.* $S(t)/S_\infty = 0.1$, about 5 h with stirring and 20 h without). However, trying to achieve signal intensities close to saturation, the incubation time has to be increased substantially for $L_0 \ll K_d$ *(for* $S(t)/S_\infty = 0.95$ about 100 h and 400 h of incubation, for stirring and non-stirring conditions, respectively).

Factor *a* varies from 0.25 to 30 for concentrations depicted on Fig. 2A and B. The development of the signal intensity strongly deviates from exponential behavior, if $a \geq 1$. In this case, Eqs. (4) or (10) should be used to describe the overall kinetics (Fig. 5A and B). The strongest deviation from single exponential behavior is expected in the limit of small $\Gamma_m \ll \Gamma_{ideal}$ and for $a \approx a_m = L_0/K_d \gg 1$, *i.e.* for such high analyte concentrations, $L_0 \gg K_d$, where the limit $S_\infty \approx S_{max}$ is attained. It is evident from Fig. 5A that the progression curve for $25 \times K_d$ concentration runs almost linearly instead of exponentially. The mass-transport limited reaction in such cases is strongly dominated by the first term in Eq. (10) and can be approximated to a large extent by linear Eq. (11) with $v_0 \approx v_m \approx k_m L_0/S_{max}$ or in direct proportionality to the mass flux. In this case, the fractional occupancy increases proportionally to the incubation time. If the condition $a < 1$ is true, the kinetics remains in single exponential regime and Eq. (7) can be used for the analysis. However, even for $\Gamma_m \ll \Gamma_{ideal}$ the binding kinetics can remain yet single exponential for $L_0 \ll K_d$, *i.e.* for sufficiently low analyte concentrations, cf. Eq. (7) with $S_\infty \approx S_{max} L_0/K_d$ and $\Gamma \approx 1/\tau_m$, where $\tau_m \approx S_{max}/(k_m K_d)$ is the characteristic time describing the mass transport to the spot. The dominating character of this regime can be seen in Fig. 5B.

3.6 Performance parameters of our system

Short time incubation (only 0.5 to 2 h) using cover slip and without stirring are very typical conditions for a microarray processing [7, 20–22]. To demonstrate how strong such parameters may influence the antibody microspot kinetics, two incubation systems were compared for three different antibodies (anti-IFNG, anti-TG and anti-KLH) (Fig. 6A). Slides from one batch were incubated under different incubation conditions with 100 μL of 100 pM of every antigen: (A) overnight (12 h) incubation under usual conditions described here (well geometry with stirring); (B) only 1 h incubation, under glass cover slip and without stirring. System B represents typical incubation conditions for protein microarrays that have been used frequently. Using system A, up to 300 times higher signal intensities could be obtained.

To find out the maximally achievable sensitivities in our system, slides spotted with three different antibodies were incubated overnight (16 h) using antigen concentrations in the range of 100 nM to 2 fM (Fig. 6B). The obtained signal intensities were normalized against the maximal signal intensity at 100 nM. For all three antibodies used, the achieved dynamic range comprises, at least, from five to six

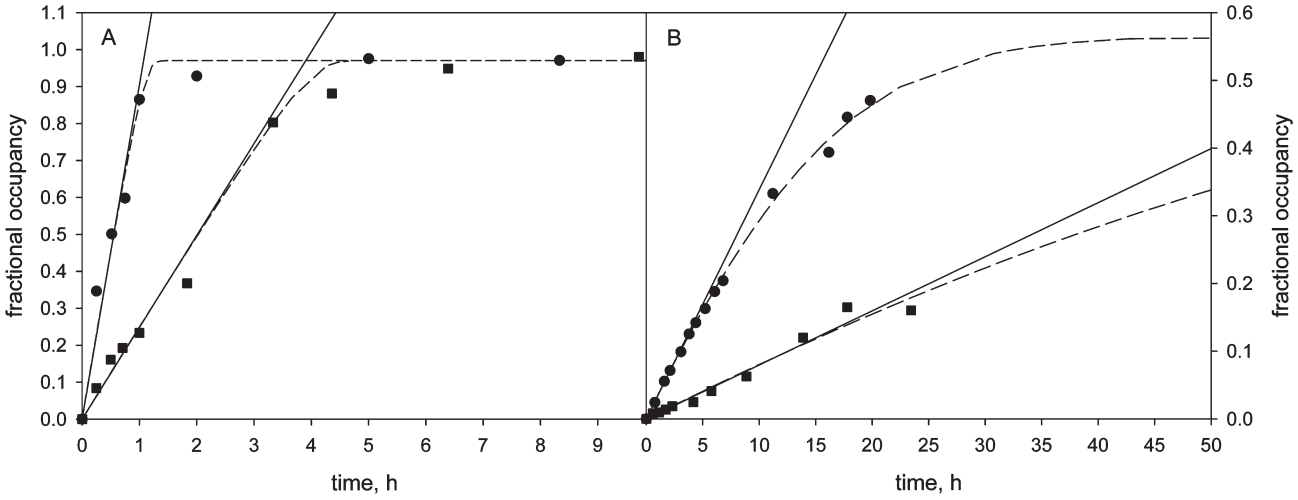

Figure 5. Development of signal intensity on an anti-IFNG spot at IFNG concentrations (A) 25 × (17 nM) and (B) 1 × (650 pM) under stirring (●) and non-stirring (■) conditions. The progression curves were fitted using Eq. (4) (–) and Eq. (11) (—). Especially at 25 × K_d, nearly complete overlap of the both equations can be observed.

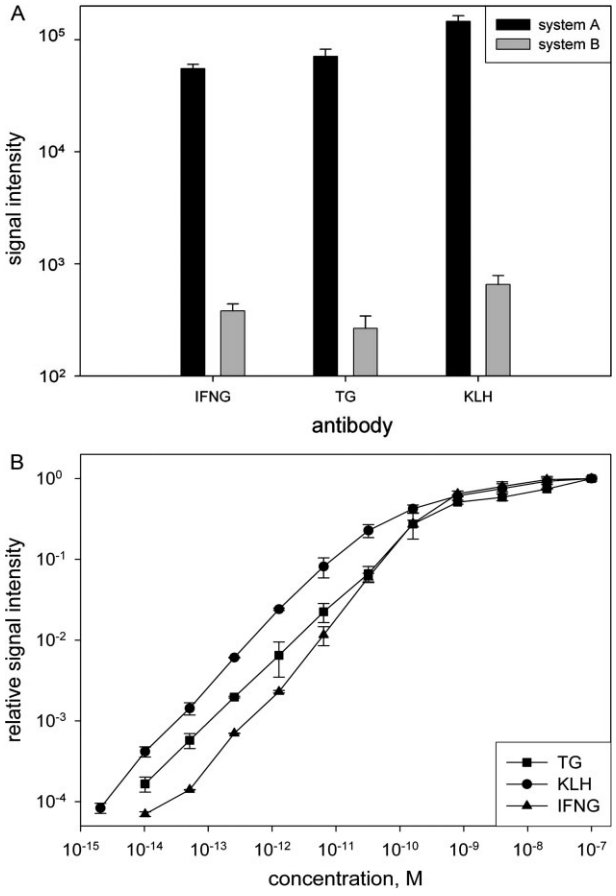

Figure 6. (A) Signal intensity for three antigen-antibody pairs achieved in our incubation system A, as described in the sections 3.2 and 3.6, and B, a commonly used incubation condition. (B) Analyte concentration/signal curves obtained after overnight incubation (12 h) are shown.

orders of magnitude. The most sensitive antigen-antibody pair was anti-KLH exhibiting a relatively high signal intensity even at concentrations of 2 fM; the detection limit for the other two antibodies, anti-IFNG and anti-TG, was about 10 fM. The lowest detectable signal intensity for anti-IFNG obtained at maximal scanner adjustment (mean signal 1956 ± 202; mean background signal 830 ± 135) was estimated to be about 2×10^4 lower as the maximal signal intensity at high L_0 set as 1. This value would correspond to only a couple of Cy3 molecules/μm^2 (personal communication with Perkin-Elmer Life and Analytical Sciences) as well as it is in a qualitative agreement with the fractional occupancy (estimated as about 2×10^{-5}) for this analyte concentration. This means that only a few IFNG molecules are bound on average per μm^2 of the detection spot (few dozen zmol of IFNG per spot), what is in fact already close to the scanner's detection limit of 0.1 Cy3 molecules/μm^2. On the other hand, at least $0.5–1 \times 10^5$ binding sites/μm^2 of anti-IFNG would be required to be able to detect only 1–2 IFNG molecules/μm^2. It is in a good agreement with our above estimation of the binding site density.

4 Discussion

Microarrays have inherently very small binding areas and, as a consequence of this, their binding kinetics depends strongly on the analyte concentration. Considering only "ideal" conditions for the case of antibodies, the kinetics for $L_0 \gg K_d$ would result in relatively short characteristic times, since the antibody on-rate constants k_+ vary from 10^3 to 10^8 (M^{-1}S^{-1}. However, antibody off-rates k_- of up to 10^{-5}s^{-1} would still lead to many hours or few days of incubation for small analyte concentrations (see Eq. (3)). Exemplifying it with our

anti-IFNG spot, signal saturated to 95% would be expected after only a few minutes at $L_0 \gg K_d$ and after about 2.5 h at $L_0 \ll K_d$.

Taking into account the effect of mass transport, the microspot kinetics looks dramatically different, since the ideal kinetics may be slowed down by several orders of magnitude (see Eqs. (5), (8), (9) and the accompanying analysis). A mass-transport independent character of the antibody microspot kinetics, which has been found in some previous studies [10, 11], was mainly deduced from the exponential shape of the progression curves. However, such a conclusion is not correct since the kinetics can stay exponential even under strong mass-transport limitations as it was clarified in this study (see also [23]). Typical microspot assays require dozens to several hundred hours to reach saturation at low analyte concentrations. In a study aimed to evaluate the performance of a microarray sandwich assay by detecting of a mixture of 24 common serum proteins [24], longer incubation times (from 1 to 18 h) have lead to a manifold increase of the signal intensities for most antibody spots. This effect was observed even with a very small sample volume (20 μL) and with subnanomolar analyte concentrations (10^{-9}–10^{-11} M). Moreover, the factors of the slowing down of the ideal kinetics ($\phi = k_+ S_{max} / k_m$; 35 and 140 for stirring and non-stirring conditions, respectively) obtained in our study may be even substantially higher in other experimental systems. This can happen due to *e.g.* smaller diffusion coefficients (for larger molecules), highly viscous buffers, incubation without mixing or under imperfect mixing (caused, *e.g.* by the geometry of the incubation chamber, or by a poor mixing device), antibodies with higher affinities, 3-D slide surfaces representing an additional diffusion barrier and other reasons. As it was demonstrated in Fig. 6B, the importance of these parameters is unfortunately strongly underestimated in the protein microarray publications. Additionally, such prolonged reaction times may be followed by strong statistical fluctuations due to a small number of the interacting molecules. A poor reproducibility of the detection has to be a consequence of this.

The mathematical tool provided here can be applied for the analysis and design of protein as well as DNA microarray experiments. It may in future also enable a comparison of different microarray systems in terms of quantitative performance parameters, like k_m, for example. Especially in the field of protein microarrays, in which the technological performance strongly depends on such parameters as diffusion coefficients, affinity or interface activities, which are related to the particular analyte/receptor molecules, it might facilitate the development of the technique. Our simple analytical solution of the TCM in terms of the special Lambert function (see Eq. (4)), or the corresponding inverse dependence in Eq. (10) allows to fit the progression curves with a few adjustable parameters only. The mass-transport dependence of the overall reaction can also be easily evaluated by fitting Eq. (11) to the initial development of signal in time. The further advantage of our approach is the possibility to evaluate the microspot reaction kinetics without any knowledge about diffusion coefficients, stirring velocity or density of binding sites, parameters, which are reflected by phenomenological values k_m and S_{max}, respectively. These equations may also be applied to analyze the bimolecular reactions in other systems such as the Biacore instrument.

It should be emphasized that the TCM assumes steady-state conditions for the analyte concentration, i.e. the analyte concentration in the immediate vicinity of the spot achieves instantly a quasi-equilibrium and follows then adiabatically to the signal development. In contrast, the reactions in the classical MTP well completely covered with receptor molecules are entirely in a non-steady-state regime and develop proportionally to $\sqrt{t}$ [25, 26]. Our theory is clearly not applicable for such situations. However, in our experiments with different antibodies, a strong deviation from the steady-state regime was observed only under non-stirring conditions for very large antigen molecules like TG (molecular weight 680 kDa) (data not shown).

Despite the fact that the antigen solution in the well is homogenized within a few seconds by the SlideBooster, the reaction velocity is accelerated only by about fourfold. Highly affine binding reactions measured, *e.g.* by Biacore systems may suffer also from mass-transport limitations in spite of a high velocity of the solution pumped through the chip. However, it is hard to imagine, that the remaining mass-transport dependence of the reaction is caused only by the mass flux from incubation solution. At present, we do not have a theoretically sound explanation of this experimental feature. We believe that a mechanism similar to the two-stage capture process described by Adam and Delbrück [27] may provide a clue. Large amphiphatic protein molecules exhibit abundant surface activities and can be weakly bound to the slide's surface by a number of interactions [28]. Adsorption capacity of different surfaces may be significant to influence the reaction kinetics. For instance, different organic or silanized surfaces can bind nonspecifically from few micrograms until few dozen nanograms/cm^2 of typical proteins such as albumin or fibrinogen [29]. Therefore, a nonspecific adsorption even on a blocked surface may significantly deplete the initial analyte concentration violating possibly the ambient analyte condition if the absorbed molecules remain immobilized. We assume however, that proteins weakly bound to surface can still migrate by a 2-D diffusion until they will be either desorbed or bind upon encountering a binding site of antibody. The interface mobility of proteins is known from the literature [30] to be in the range of 10^{-7}–10^{-10} cm^2/s.

Summarizing these facts and assumptions, we hypothesize the following reaction mechanism: the initial analyte concentration L_0 may be first separated into the two-analyte pools, the bulk solution and the interface portion; the both phases exchange continuously by the analyte molecules as well as may directly provide the analyte for the binding process on the spot in a steady-state regime. Moreover, both mechanisms may occur in a sequence. Namely, the analyte

molecule first reaches the surface of the spot either from the bulk, or from the surrounding surface and then searches diffusionally within the spot until it finds the antibody molecule to bind with. A restriction on the further increase of the reaction velocity by intensive stirring which we observed experimentally may be imposed namely by the 2-D diffusion, which is not (or only slightly) influenced by stirring in bulk. The capture of analyte molecules from the surface seems to be also one of the main mechanisms in the kinetics of the related DNA-microarrays [31].

In the context of practical consequences, the influence of different factors such as the mixing device performance, surface chemistry, incubation buffers and such alike on the binding kinetics can be easily deduced from the signal development in time by measuring the initial slope of the corresponding progression curve. On the other hand, simple comparison of signal intensities, often practiced in the microarray field, may lead, however, to erroneous conclusions about the appropriateness of one, or another particular set of the parameters. If, *e.g.* two systems vary only by their mass-flux conditions, the differences in performance might be underestimated due to an earlier saturation of the signal intensity. Furthermore, if one system has higher k_m but lower binding site density than another one, one may obtain controversial results from different experiments depending on the used concentration L_0 and the incubation time. On the other hand, if k_m are comparable in different systems, potential advantages could be demonstrated only by longer incubation times or higher analyte concentrations. Furthermore, comparing different receptor molecules within a microarray based antibody screening or protein-protein interaction studies, it is difficult to expect any strong correlation with the K_d of the analyzed molecules at short incubation times due to the proportionality of the initial signal development to either k_+ or k_m in the reaction or mass flux limits, respectively. It is also clear that suitability and appropriateness of an array of microarray assay parameters like immobilization strategy, design criteria (spot size and shape, binding sites density, spotting pattern), incubation parameters (chamber, time, sample concentration and volume, stirring), detection approach (direct, sandwich or signal amplification systems) has to be systematically considered from the viewpoint of the mass-transport limited kinetics. A more detailed theoretical and experimental analysis of different fabrication parameters such as spot size, binding sites density, incubation geometry, *etc* is currently in progress.

We have revealed a crucial role played by the mass-transport effects in a typical antibody microspot assay. A strong mass-transport dependence of the microarray reactions seems to be the main physical limitation of this technology. To reduce it as much as possible by analysis and optimization of multiple parameters listed above, to optimize the assay in context of such complex kinetics and finally to define an optimal for particular system incubation time should be maybe the most important issues in designing microarrays. This can improve absolute signal as well as signal-to-noise ratios opening perspectives for further sensitivity improvement using, *e.g.* a signal amplification system. Using a highly sensitive sandwich detection approach (anti-biotin coated resonance light scattering (RLS) gold particles directed against biotinylated secondary antibodies), Saviranta *et al.* [24) could improve the detection limit for big part of spotted antibodies by factor 2–15 only due to significantly prolonged incubation times. The achieved by these authors detection limits (24 antibodies) varied between few fM until low pM range. The sensitivity achieved by us in the low femtomolar range as well as the detection range of more than five orders of magnitude seems to be maximally attainable within our system, because, due to exponential character of the progression curves, the signal intensity at low L_0 can be only redoubled at much longer incubation times. These performance parameters indicate, however, that the capacity of this new technology is not fully exploited at present. Our main conclusion is that a good understanding of microarray reaction kinetics is paramount for optimizing microarray assays.

We thank David G. Wild for valuable discussions and his comments on the manuscript. The work was funded by grants of the German Federal Ministry of Education and Research (BMBF) as part of the programs Proteomics, DHGP, NGFN as well as the European Commission.

5 References

[1] Ekins, R. P., *Clin. Chem.* 1998, *44*, 2015–2030.

[2] Ekins, R., Chu, F., *TIBTECH* 1994, *12*, 89–94.

[3] MacBeath, G., *Nat. Genet.* 2002, *32*, 526–532.

[4] Kusnezow, W., Pulli, T., Witt, O., Hoheisel, J. D., in Schena, M. (Ed.), *Protein Microarrays*, Jones and Bartlett Publishers, Sudbury 2004, pp. 247–284.

[5] Kusnezow, W., Hoheisel, J. D., *J. Mol. Recognit.* 2003, *16*, 165–176.

[6] Miller, J. C., Zhou, H., Kwekel, J., Cavallo, R., Burke, J., Butler, E. B., Teh, B. S., Haab, B. B., *Proteomics* 2003, *3*, 56–63.

[7] Knezevic, V., Leethanakul, C., Bichsel, V. E., Worth, J. M., Prabhu, V. V., Gutkind, J. S., Liotta, L. A. *et al.*, *Proteomics* 2001, *1*, 1271–1278.

[8] Sreekumar, A., Nyati, M. K., Varambally, S., Barrette, T. R., Ghosh, D., Lawrence, T. S., Chinnaiyan, A. M., *Cancer Res.* 2001, *61*, 7585–7593.

[9] Butler, J. E., *Methods* 2000, *22*, 4–23.

[10] Sapsford, K. E., Liron, Z., Shubin, Y. S., Ligler, F. S., *Anal. Chem.* 2001, *73*, 5518–5524.

[11] Xu, Y., Bao, G., *Anal. Chem.* 2003, *75*, 5345–5351.

[12] Adey, N. B., Lei, M., Howard, M. T., Jensen, J. D., Mayo, D. A., Butel, D. L., Coffin, S. C. *et al.*, *Anal. Chem.* 2002, *74*, 6413–6417.

[13] Liu, R. H., Lenigk, R., Druyor-Sanchez, R. L., Yang, J., Grodzinski, P., *Anal. Chem.* 2003, *75*, 1911–1917.

[14] Toegl, A., Kirchner, R., Gauer, C., Wixforth, A., *J. Biomol. Tech.* 2003, *14*, 197–204.

[15] Schuck, P., *Biophys. J.* 1996, *70*, 1230–1249.

[16] Schuck, P., Minton, A. P., *Anal. Biochem.* 1996, *240*, 262–272.

[17] Schuck, P., *Curr. Opin. Biotechnol.* 1997, *8*, 498–502.

[18] Goldstein, B., Coombs, D., He, X., Pineda, A. R., Wofsy, C., *J. Mol. Recognit.* 1999, *12*, 293–299.

[19] Corless, R. M., Gonnet, G. H., Hare, D. E. G., Jeffrey, D. J. & Knuth, D. E., *Adv. Comput. Math.* 1996, *5*, 329–359.

[20] Joos, T. O., Schrenk, M., Hopfl, P., Kroger, K., Chowdhury, U., Stoll, D., Schorner, D. *et al.*, *Electrophoresis* 2000, *21*, 2641–2650.

[21] Haab, B. B., Dunham, M. J., Brown, P. O., *Genome. Biol.* 2001, *2*, research0004.10004.10013.

[22] Angenendt, P., Glokler, J., Murphy, D., Lehrach, H., Cahill, D. J., *Anal. Biochem.* 2002, *309*, 253–260.

[23] Schuck, P., Minton, A. P., *TIBS* 1996, *21*, 458–460.

[24] Saviranta, P., Okon, R., Brinker, A., Warashina, M., Eppinger, J., Geierstanger, B. H., *Clin. Chem.* 2004, *50*, 1907–1920.

[25] Stenberg, M., Nygren, H., *J. Theor. Biol.* 1985, *113*, 589–597.

[26] Stenberg, M., Nygren, H., *J. Immunol. Methods* 1988, *113*, 3–15.

[27] Adam, G., Delbrück, M., *Reduction of Dimensionality in Biological Diffusion Process,* W. H. Freeman&Company, Publishers, San Francisco 1968.

[28] Hlady, V. V., Buijs, J., *Curr. Opin. Biotechnol.* 1996, *7*, 72–77.

[29] Tengvall, P., Lundstrom, I., Liedberg, B., *Biomaterials* 1998, *19*, 407–422.

[30] Zhdanov, V. P., Kasemo, B., *Proteins* 2000, *39*, 76–81.

[31] Chan, V., Graves, D. J., McKenzie, S. E., *Biophys. J.* 1995, *69*, 2243–2255.

